# Mechanical and electronic properties of SiC nanowires: an *ab initio* study

J. B. Oliveira,[1,2] J. M. Morbec,[3,a)] and R. H. Miwa[1]

[1)] *Instituto de Física, Universidade Federal de Uberlândia, Caixa Postal 593, CEP 38400-902, Uberlândia, MG, Brazil*

[2)] *Instituto Federal do Triângulo Mineiro, CEP 38305-200, Ituiutaba, MG, Brazil*

[3)] *Faculty of Physics, University of Duisburg-Essen, Lotharstrasse 1, 47057 Duisburg, Germany*

(Dated: 24 October 2019)

Using first-principles calculations, based on density functional theory, we have investigated the mechanical and electronic properties of hydrogen-passivated 3C-, 2H-, 4H-, and 6H-SiC nanowires, analyzing the effects of the diameter on these properties. Our results show that the band-gap energies of the nanowires are larger than the corresponding bulk values, and decrease with the increasing diameter. All nanowires investigated exhibit direct band gaps, in contrast with the indirect band gaps observed in bulk SiC. The effect of uniaxial stress on the electronic properties of SiC nanowires has been also examined, and our results reveal that the band-gap dependence on the strain is different for each nanowire polytype. In 3C-SiC nanowires, the band gaps increase (decrease) with tensile (compressive) strain. For 4H- and 6H-SiC nanowires the influence of strain on the band gaps is more pronounced in the thicker wires. Finally, we estimated the band offsets of hypotetical NW homostructures, composed by stacking SiCNW layers with different polytypes.

PACS numbers: 62.25.-g, 73.22.-f, 71.15.Mb, 71.15.Nc

## I. INTRODUCTION

One-dimensional silicon carbide (SiC) nanostructures have attracted increasing attention in the last years owing to their great potential for nanotechnology applications. These nanostructures combine the outstanding properties of SiC (high thermal conductivity, excellent chemical stability, high electron drift velocity, high breakdown electric field, good field-emitting performance, and others) with quantum-size effects, and are promising materials for the fabrication of electronic and optoelectronic nanodevices.

Among the different SiC nanostructures, SiC nanowires (NWs) are particularly interesting because they exhibit exceptional optical, electronic, chemical, and mechanical properties. These NWs have been synthesized using different methods in recent years[1–8] and are expected to have great potential for use in light-emitting diodes and field-emission displays due to their good photoluminescence[9–11] and field-emission[3,7,12,13] properties. Moreover, SiCNWs present high strength and elasticity,[14] besides an unusual large strain plasticity at low temperatures,[15] and could be used as reinforcing elements in composite materials.[16,17]

Many characteristics of the SiCNWs are strongly related to their low dimensionality. For this reason, it is important to study the effects of quantum confinement on the properties of these systems. Rurali[18] investigated (using first-principles calculations) the electronic properties of pure and hydrogen-passivated 3C-SiCNWs[19] grown along the [110] direction, and showed that pure NWs present metallic character due to surface reconstructions, whereas quantum confinement induces a gap-broadening effect in hidrogenated NWs. In another theoretical work, Durandurdu[20] observed that the band gaps of pure wurtzite SiCNWs increase with increasing diameters, in contrast to hydrogenated wurtzite SiCNWs whose band gaps decrease with increasing diameters. Using first-principles calculations, Yan *et al.*[21] investigated the effect of uniaxial stress on the electronic properties of hydrogen-passivated [111] 3C-SiCNWs. They verified that these NWs have direct band gaps, and that their band gaps increase with increasing tensile stress or with decreasing diameters. Meanwhile, Wang *et al.*[22] performed first-principles calculations to study the energetic stability and electronic properties of hydrogenated [110]-, [111]-, and [112]-oriented 3C-SiCNWs, and [0001]-oriented 2H-SiCNWs. They verified that the energetic stability of the SiCNWs depends on their orientation and that 3C-SiCNWs oriented along the [111] direction are the most favorable ones. In addition, they observed that the band gaps of the NWs decrease with increasing diameters, and that [112]-oriented 3C-SiCNWs have indirect band gaps (similar to bulk SiC), while the other NWs have direct band gaps.

In this work we have investigated, using *ab initio* calculations, the effects of the reduced dimensionality on the electronic and mechanical properties of SiCNWs. We considered SiCNWs constructed from the cubic (3C or $\beta$) and hexagonal (2H, 4H, 6H) polytypes, oriented along the [111] and [0001] directions, respectively. We have analyzed the dependence of the Young's moduli and the band-gap energies of the nanowires on their diameters, as well as the influence of uniaxial stress on their electronic properties. By considering a set of stacking sequences of different SiC polytypes, we estimate the band offsets of hypothetical SiCNW homostructures.

[a)] Electronic mail: jmmorbec@gmail.com

## II. COMPUTATIONAL METHODS

Our calculations were performed within the framework of the density functional theory (DFT),[23] as implemented in the SIESTA code,[24] employing norm-conserving fully separable Troullier-Martins pseudopotentials[25] to describe the electron-ion interactions and the local density approximation (LDA)[26,27] for the exchange-correlation functional. The Kohn-Sham orbitals were expanded in a linear combination of numerical pseudoatomic orbitals,[28] with an energy shift of 0.20 eV. We used a double-zeta basis set for H atoms (H atoms were employed to passivate the surface dangling bonds) and double-zeta with polarization functions for Si and C atoms. A mesh cutoff energy of 170 Ry was used for the real space grid integration. The nanowires were modeled within the supercell approach, using a vacuum region of about 10 Å between the wires in the radial direction. All the atomic positions were allowed to relax during the geometry optimization until the Hellman-Feynman forces were less than 0.05 eV/Å for 2H-SiCNWs and 0.02 eV/Å for the other NWs. The Brillouin zone was sampled using 1 **k**-points for 3C-, 4H-, and 6H-SiCNWs, and 2 **k**-points for 2H-SiCNWs. The convergence of the $k$-point grid was examined for the 3C-SiCNWs: considering up to 14 $k$-points, we did not find any change in the cohesive energy or in the band gap of these systems.

## III. RESULTS AND DISCUSSION

### A. SiC bulk

We initially examined the structural, mechanical, and electronic properties of bulk 3C-, 2H-, 4H-, and 6H-SiC. Our results for optimized lattice constants, Young's moduli, band gap energies, and cohesive energies are presented in Table I. The cohesive energies per atom, $E_c$, and the Young's moduli, $Y$, were estimated using the equations,

$$E_c = \frac{\sum_i n_i E_i - E}{\sum_i n_i} \tag{1}$$

and

$$Y = \frac{1}{V}\left(\frac{d^2E}{d\epsilon^2}\right)_{\epsilon=0}, \tag{2}$$

where $E$ is the total energy, $n_i$ is the number of atoms of specie $i$ ($i$=Si/C for bulk, and $i$=Si/C/H for NW), $E_i$ is the energy of the isolated atom, $\epsilon$ is the strain, and $V$ is the equilibrium volume.

Our calculated cohesive energies (Table I) indicate that the 2H structure (which has the lowest $E_c$) is the most unstable structure among the polytypes investigated, whereas 4H and 6H are the most stable ones. This is consistent with previous theoretical works[36,37] and with the fact that the 2H polytype is rarely observed. We noted that our result for $E_c$ of bulk 3C-SiC ($E_c^{3C}$ = 6.778 eV/atom) is larger than the experimental value, 6.34 eV/atom[32] [see Table I]; comparing with previous theoretical studies, (i) Chang and Cohen[38] obtained $E_c^{3C}$ = 6.66 eV/atom, and (ii) Jiang *et al.*[39] obtained 6.40 eV/atom, both calculations were performed within the DFT approach, the former using plane waves as a basis set, while the latter used atomic orbitals.

In our electronic-structure calculations, we found indirect band-gaps of 1.31, 2.69, 2.20, and 2.00 eV for bulk 3C-, 2H-, 4H-, and 6H-SiC, respectively. These results are underestimated by more than 30% with respect to the experimental values [see Table I], which is common in DFT calculations, but are in good agreement with previous theoretical results: for example, using DFT calculations (i) Persson and Lindefelt[41] found 1.30, 2.11, 2.17 and 1.97 for $E_g$ of bulk 3C-, 2H-, 4H-, and 6H-SiC, respectively, and (ii) Wang *et al.*[42] obtained 1.37, 2.78, 2.36, and 2.14 eV.

### B. SiC nanowires

#### 1. Cohesive energy and Young's modulus

Next, we studied 3C-SiCNWs oriented along the [111] direction, and 2H-, 4H-, and 6H-SiCNWs oriented along the [0001] direction. In order to investigate the diameter dependence of the electronic and mechanical properties of these systems, we considered NWs with different diameters, $d$, as depicted in Fig. 1. We studied 3C-, 2H-, 4H- and 6H-SiCNWs with $d \approx 0.71$, 1.07, and 1.42 nm. The dangling bonds at the nanowire surfaces were passivated by H atoms to eliminate the surface states and prevent surface reconstruction. We found optimized Si-C bond lengths from 1.87 to 1.90 Å; the Si-H and C-H bond lengths at the surfaces are about 1.52 and 1.12 Å, respectively.

The cohesive energy of each nanowire ($E_c^{NW}$), calculated using Eq. (1), is presented in Table II. For all types of nanowires, the values of $E_c^{NW}$ are smaller than the corresponding bulk values ($E_c^{bulk}$) [see also Table I], but increase and approach to $E_c^{bulk}$ with increasing diameters. We also noted that the 2H-SiCNWs have the largest cohesive energies, which suggests that 2H-SiCNWs are more stable than 3C-, 4H-, and 6H-SiCNWs with similar diameters. This result contrasts with that obtained for bulk SiC [Table I] that indicates that 2H is the less stable polytype. Our results are consistent with the theoretical work of Ito *et al.*,[43] in which 2H was predicted to be the most stable structure for SiCNWs with $d < 20$ nm, but do not agree with the *ab initio* study performed by Wang *et al.*,[22] in which SiC nanowires with $d < 2.8$ nm were investigated and [111] 3C-SiCNWs were found to be more stable than [0001] 2H-SiCNWs. Ito *et al.*[43] attributed the instability of the 3C-SiCNWs with $d < 20$ nm to the large number of dangling bonds at their surfaces, when

TABLE I. Calculated equilibrium lattice constants, bulk moduli ($B_o$), band gap energies ($E_g$), and cohesive energies ($E_c^{\rm bulk}$) of bulk 3C-, 2H-, 4H-, and 6H-SiC. The values in parentheses are experimental data taken from Refs. 31–33.

| | lattice constants (Å) | $B_o$ (GPa) | $E_g$ (eV) | $E_c^{\rm bulk}$ (eV/atom) |
|---|---|---|---|---|
| 3C-SiC | $a = 4.35$ ($4.36^{\rm a}$) | 219.1 (224.0) | 1.31 ($2.39^{\rm a}$) | 6.778 ($6.34^{\rm b}$) |
| 2H-SiC | $a = 3.08$ ($3.08^{\rm a}$) | 207.8 (223.4) | 2.69 ($3.33^{\rm a}$) | 6.619 |
| | $c = 5.02$ ($5.05^{\rm a}$) | | | |
| 4H-SiC | $a = 3.07$ ($3.07^{\rm a}$) | 209.0 (223.4) | 2.20 ($3.26^{\rm a}$) | 7.208 |
| | $c = 10.07$ ($10.05^{\rm a}$) | | | |
| 6H-SiC | $a = 3.08$ ($3.08^{\rm a}$) | 209.2 (223.4) | 2.00 ($3.02^{\rm a}$) | 7.208 |
| | $c = 15.09$ ($15.12^{\rm a}$) | | | |

[a] Ref. 31
[b] Refs. 32,33

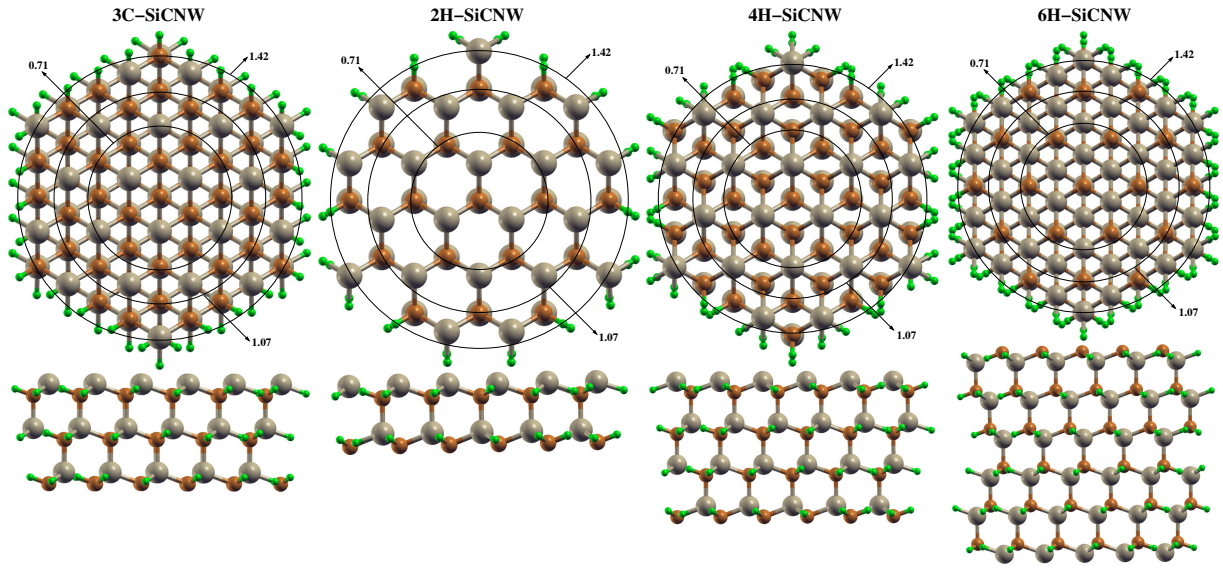


FIG. 1. (Color online) Cross-section (top panel) and side (bottom panel) views of the 3C-SiCNWs oriented along the [111] direction, and 2H-, 4H-, and 6H-SiCNWs oriented along the [0001] direction. The circles indicate the different diameters considered in each case (the diameters are in nm). Side view is shown for the thickest nanowire.

compared to 2H-SiCNWs. Here we found, however, that 3C-SiCNWs are also less stable than 2H-SiCNWs when the surface dangling bonds are passivated by H atoms. The reduction of the cohesive energy in the NWs can be attributed to the formation of surface dangling bonds, which is proportional to the NW surface area ($\propto d$). Whereas the SiC bulk contribution, which is proportional to the NW volume ($\propto d^2$), increases the cohesive energy, being $E_c^{\rm bulk}$ its upper limit, that is, we can infer that the former contribution reduces for larger diamenters, where $E_c^{\rm NW} \rightarrow E_c^{\rm bulk}$.

In Table II, we also present our results for the Young's moduli of SiCNWs, determined according to Eq. (2), with strains from -4% to +4% along the axial direction. We note that, for all nanowires investigated, the Young's moduli decrease with the increasing diameter. This behavior is similar to that observed in Ag[44,45], Pb[45], and (more recently) for GaAs[46] nanowires, but is opposite to that found in InAs,[47] InP,[47] Si,[48?] and Ge[50] nanowires. There is a dependence of the Young's moduli on the nanowire diameter, which is larger for the hexagonal nanowires (the Young's modulus of 2H-, 4H- and 6H-SiCNWs reduces by ∼12, 15, and 19% by increasing the NW diameter from 0.71 to 1.42 nm). Similar dependence between the Young's modulus and the NW diameter has been observed for GaAs NWs: Chen et al.[46] found a reduction of ∼15% (189→161 GPa) in the Young's modulus of wurtzite GaAs NWs by increasing the NW diameter from 75 to 170 nm (∼126%). Meanwhile, as shown in Table II, the Young's modulus of 3C-SiCNW is less sensitive to the diameter: while the diameter increases by a factor of 2 (0.71→1.42 nm), the Young's modulus decreases only by about 5.3% (642→608 GPa). This behavior observed for 3C-SiCNW is consistent with previous theoretical works,[21,51] and our calculated Young's moduli for 3C-SiCNW are in good agreement with the values

TABLE II. Calculated cohesive energies ($E_c^{\rm NW}$), band gap energies ($E_g$), and Young's moduli ($Y$) for 3C-, 2H-, 4H-, and 6H-SiCNWs as functions of diameter $d$.

| $d$ (nm) | $E_c^{\rm NW}$ (eV/atom) | $E_g$ (eV) | $Y$ (GPa) |
|---|---|---|---|
| 3C-SiCNW | | | |
| 0.71 | 5.07 | 3.24 | 642.03 |
| 1.07 | 5.49 | 2.62 | 617.70 |
| 1.42 | 5.72 | 2.17 | 608.00 |
| 2H-SiCNW | | | |
| 0.71 | 5.30 | 3.94 | 581.21 |
| 1.07 | 5.61 | 3.29 | 523.24 |
| 1.42 | 6.17 | 2.97 | 494.60 |
| 4H-SiCNW | | | |
| 0.71 | 5.22 | 3.90 | 563.65 |
| 1.07 | 5.35 | 3.39 | 494.14 |
| 1.42 | 5.70 | 3.02 | 480.59 |
| 6H-SiCNW | | | |
| 0.71 | 5.07 | 3.77 | 584.56 |
| 1.07 | 5.35 | 3.11 | 540.08 |
| 1.42 | 5.71 | 2.76 | 472.33 |

obtained by Yan *et al.*[21] using DFT calculations. Our calculated Young's moduli for the nanowires are larger than 300 GPa, which indicates that SiC nanowires are more rigid than Si[48,49] and Ge[50] nanowires grown along the same direction and with similar diameters.

In NW systems, we can infer that there are two contributions to the Young's moduli, one from the NW surface, and another from the inner (bulk) region of the NW. In this case, the relative contribution of each term is proportional to the surface/bulk ratio, namely $1/d$. Within such a scenario, our results indicate that the NW surfaces contribute to increase the Young's moduli of SiCNWs, since the surface effects are strenghtened for NWs with smaller diameters. On the other hand, by increasing the NW diameter, the role played by the surface becomes less important, and the Young's moduli becomes ruled by the bulk region of the NW. However, it is worth noting that such a surface/bulk dependence is commited to the NW bulk material, and its surface properties. For instance, the Young's modulus of Ge (GaAs) NWs increases (decreases) by increasing the NW diameter.[46,50]

### 2. Electronic properties

Our electronic structure calculations reveal that all nanowires investigated have direct band gaps at Γ point, in contrast with the indirect band gaps observed in bulk SiC. We note that the band-gaps of the nanowires [Table II] are larger than those of their counterpart bulk phases [see Table I]. These results indicate strong effects of the quantum confinement on the electronic properties of the nanowires. It is interesting to note that 3C is the structure with the narrowest band gap among the nanowires investigated, and also among the different polytypes for bulk SiC [see Table I]. Our results for 3C- and 2H-SiCNWs are consistent with previous theoretical works.[20–22]

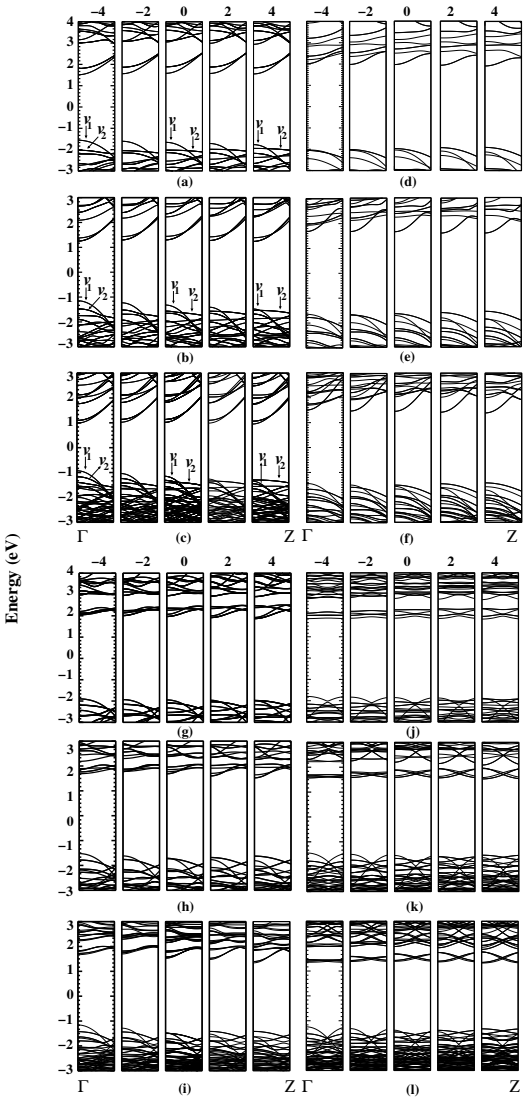


FIG. 2. Electronic band structures for (a)–(c) 3C-, (d)–(f) 2H-, (g)–(h) 4H- and (j)–(l) 6H-SiCNWs with diameters of 0.71, 1.07, and 1.42 nm.

In addition, we have investigated the effects of strain on the electronic properties of SiCNWs. All nanowires were strained from -4% (compressive) to +4% (tensile) strain, with increments of 1%. In Fig. 2 we present the electronic band structures of the SiCNWs for wave vector along

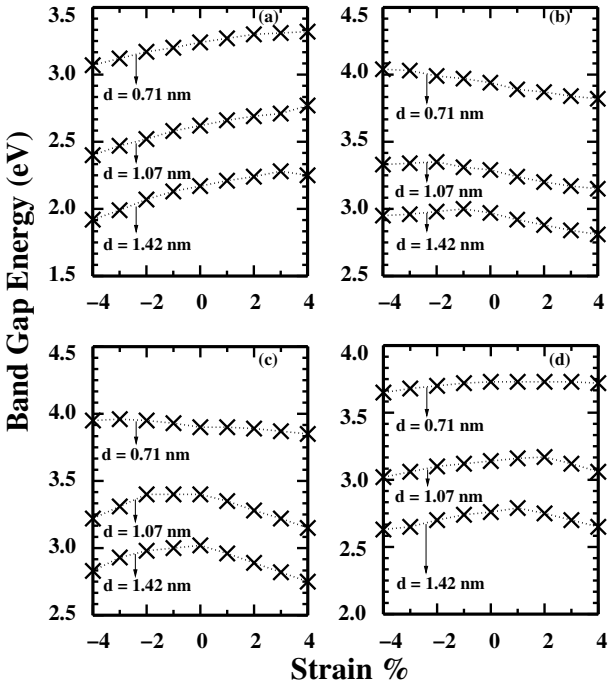


FIG. 3. Band gap energies (in eV) as a function of the strain (in %) for (a) 3C-, (b) 2H-, (c) 4H-, and (d) 6H-SiCNWs.

the NW growth direction. We verify that, in general, the main features of the electronic band structure have been preserved upon external strain; however there are some changes that are worth being reported. The highest occupied states, at the Γ-point, of the the 3C-SiCNW is characterized by a light-hole (LH) band followed by a heavy-hole (HH) band, $v1$ and $v2$ in Figs. 2(a)–2(c). The energy difference between $v1$ and $v2$ (at the Γ-point) increases (decreases) by compressing (stretching) the NW. For the thinnest 3C-SiCNW, even for a strain of +4%, $v1$ lies above $v2$; however, such an energy difference reduces by increasing the NW diameter. For the largest diameter, a valence band crossing between $v1$ and $v2$ takes place by stretching the NW. Indeed, similar behavior has been verified for the other SiCNWs. Those findings allow us to infer that, upon tensile strain, the hole mobility will be reduced, since the edge of the valence band becomes characterized by HH states ($v2$). On the other hand, by compressing the SiCNWs, we find LH states ($v1$) at edge of the valence band. For instance, by calculating the hole effective masses ($m_h^*$), defined as $\hbar^2(\frac{\partial^2 E}{\partial k^2})^{-1}$, we obtained $m_h^* \approx 0.5m_0$ ($m_0$ is the free electron rest mass) for the 3C-SiCNW with a diameter of 1.42 nm; by stretching the NW by +4%, $m_h^*$ increases to $5.3m_0$. Focusing on the conduction bands, we verify that the lowest unoccupied states of 4H- and 6H-SiCNWs become less localized by stretching the NWs from −4% to +4%. For instance, in the 4H-SiCNW (with $d$=1.42 nm) compressed by −4%, the lowest unoccupied states lie in an energy interval of ∼0.2 eV [Fig. 2(h)]; while the strained NW (to +4%) presents an energy dispersion ∼0.6 eV, reducing the electron effective mass ($m_e^*$). Here, $m_e^*$ reduces from $1.1m_0$ (strain = −4%) to $0.3m_0$ by applying a tensile strain (strain> 0). Such a delocalization of the lowest unoccupied states has not been verified for the 3C- and 2H-SiCNWs, Figs. 2(a)–2(c), and 2(d)–2(f), respectively. The dispersion of those energy bands has been preserved for the different NW diameters and strains. Those systems present lower effective masses, weakly dependent on the external strain. For example, the $m_e^*$ of 3C-SiCNW with $d$=1.42 nm varies from $0.40m_0$ to $0.36m_0$ for external strain of −4% to +4%, respectively.

As can be seen in Fig. 3, the dependence between the band-gap energies and the strain is different for each nanowire type. For example, we found that the band gaps of 3C-SiCNWs with $d \approx 0.71$ and 1.07 nm [Fig. 3(a)] exhibit a monotonic behavior, increasing (decreasing) with tensile (compressive) stress. On the other hand, the band gap energies of 2H-SiCNWs [Fig. 3(b)] decrease with tensile stress (0 to +4%). For the hexagonal 4H and 6H nanowires we note that the influence of strain on the band gaps is small in the thinnest nanowires and it is more pronounced in the thickest wires; for instance, the band gap of 4H-SiCNW with $d \approx 0.71$ nm decreases only by 1.28% under tensile strain of 4% [Fig. 3(c)], while the band gap of the thicker 4H-SiCNW ($d \approx 1.42$ nm) decreases by 8.94% under similar condition. In order to provide a more complete picture of those changes in the SiCNW band-gap as a function of the NW diameter and the external strain, we next compare the energy positions of the valence band maximum (VBM) and the conduction band minimum (CBM), by considering a common energy reference. Here, following the procedure proposed by Beckman *et al.*,[57] the VBM and the CBM were lined up with respect to the energy position of the highest occupied state of an isolated $H_2$ molecule within our supercell approach. Our results, presented in Fig. 4, show that (i) the increase of the energy gap in 3C-SiCNW, strained from −4% to +4%, is mostly ruled by the downshift of the VBM, whereas the CBM is weakly perturbed [Fig. 4(a)]. In contrast, (ii) the downshift of the CBM by stretching the 2H- and 4H-SiCNWs from 0 to +4% [Figs. 4(b) and 4(c)] rules the band-gap reduction in those NWs; and (iii) for the 6H-SiCNW with larger diameters (1.07 and 1.42 nm), the increase of the energy gap by stretching the NW from −4% to around 1% is mainly dictated by the changes on the energy position of the VBM.

Stacking faults (SF) play an important role in the electronic properties of SiCNWs[39,58]. In a recent experimental work, Kuang and Cao[59] verified that SFs in 3C-SiCNWs promote the electron-hole separation along the NW, since the formation the SFs are characterized by 2H polytypes embedded in the 3C host, namely SFs give rise to a homostructure of SiCNW composed by two different stacking sequences. They found a type-II band alignment for nanowires with diameters in the range of 50 to 200 nm, with electrons/holes in the 3C/2H regions. Type-II confinement has been also verified in homojunctions of InP NWs composed by a single layer of zincblend

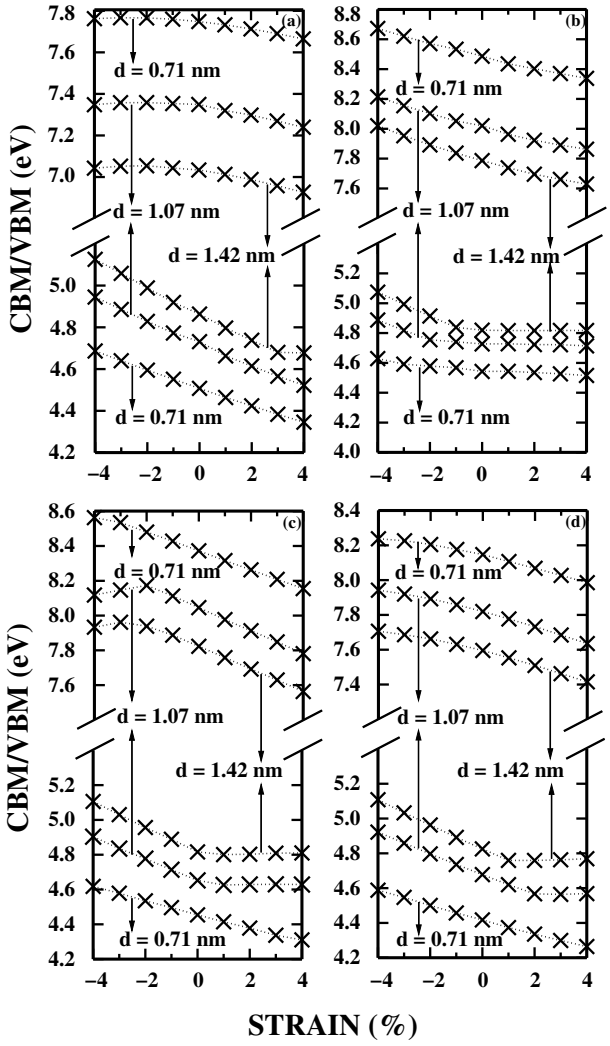


FIG. 4. Energy positions of the CBM and VBM as a function of the strain for (a) 3C-, (b) 2H-, (c) 4H- and (d) 6H-SiCNWs. The VBM and the CBM were lined up with respect to the energy position of the highest occupied state of an isolated $H_2$ molecule within our supercell approach.[57]

(zb) region embedded in the InP wurtzite (wz) host.[60] Further first-principles calculations supported the type-II band offset in wz/zb-InP NWs.[61] The band alignment may depend, however, on the width of each stacking (polytype) region as well as on the NW diameter. Indeed, such a diameter dependence has been verified in a recent *ab initio* study[62] on cubic/hexagonal Si NW homojunctions, in which type-I band alignment was found for nanowires with diameters of 1.0 and 1.8 nm, whereas type-II band offset was obtained for thicker nanowires with diameter of 3.2 nm.

Here, based on the energy positions of the VBM and CBM of the SiCNWs, as shown Fig. 4, we can infer the band offsets for different combinations of SiCNWs with similar diameters, namely giving rise to SiCNW homostructures composed by different stacking sequences. For NWs with $d \approx 1.07$ nm, for instance, the VBM of

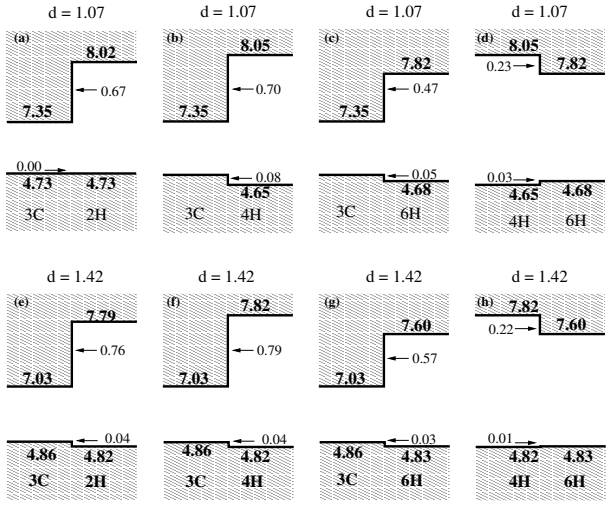


FIG. 5. Schematic model of (a+e) 3C/2H-, (b+f) 3C/4H-, (c+g) 3C/6H-, and (d+h) 4H/6H-SiCNWs homojunctions. Top panels: $d \approx 1.07$ nm for 3C-, 2H-, 4H-, and 6H-SiCNWs. Bottom panels: $d \approx 1.42$ nm for 3C-, 2H-, 4H-, and 6H-SiCNWs.

2H- and 3C-SiCNWs have the same energy, while the CBM of 2H lies 0.67 eV above the CBM of 3C-SiCNW, resulting in a valence (conduction) band offset of 0.00 (0.67) eV, as depicted in Fig. 5(a). We noticed, additionally, that there is a dependence between the band offsets and the NW diameters: by increasing the diameter of 3C/2H-SiCNWs from 1.07 to 1.42 nm, the valence and conduction band offsets increase from 0.00 to 0.04 eV and from 0.67 to 0.76 eV, respectivelly [see Figs. 5(a) and (e)], giving rise to a type-I band alignment. As we mentioned in the previous paragraph, an experimental study by Kuang and Cao[59] reported type-II band offset for thick (50–200 nm) 3C/2H-SiCNW homojunctions; this suggests that SiC NWs may have the same behavior as observed for cubic/hexagonal Si NW homojunctions,[62] with type-I alignment for thin nanowires and type-II band offset for thick nanowires. Further investigations are necessary to clarify the dependence of band offsets, in SiCNW homojunctions, with (i) the NW diameter (by considering larger diamenters), and (ii) the width of the different stacking regions.

We are aware that this an estimation since we are not taking into account the charge transfers (dipole effects) at the interfaces. Such a charge transfer should be small since we have the same atomic elements at the both sides of the interface. In this case, the intrinsic properties of the bulk phase, *viz.*: energy band-gap, ionization potential, and electronic affinity, will play the major role in the band alignment. Thus, the general trends of the band offsets, for different polytype combinations, can be inferred through the electronic properties of the separated NWs.

Further VBM/CBM energy level comparison allows us to infer that the 3C/4H- and 3C/6H-SiCNWs will present a type-I band alignment, Figs. 5(b+f) and 5(c+g), with

both electrons and holes confined in the 3C-SiCNW. Those predictions are reasonable, since the energy gaps of 4H-, and 6H-SiC bulk phase are larger when compared with the one of 3C-SiC bulk. Finally, by combining the 4H and 6H stacking, Figs. 5(d) and (h), we can infer an electron localization in the 6H region (CBM≈0.2 eV), and delocalized hole states (VBM≈0).

## IV. SUMMARY

In summary, we performed first-principles calculations to investigate the effects of the diameter on the mechanical and electronic properties of hydrogen-passivated [111] oriented 3C-, and [0001] oriented 2H-, 4H-, and 6H-SiCNWs. Our results show that the Young's moduli and the band gaps of the nanowires are larger than those of their counterpart bulk phases, and decrease with the increasing diameter. All nanowires exhibit direct band gaps, in contrast with the indirect band gaps observed in bulk SiC, and 3C-SiCNWs have the narrowest band gap among the nanowires investigated. We also examined the effect of uniaxial stress on the electronic properties of these nanowires; our results reveal that the band-gap dependence on the strain is different for each nanowire type. Under tensile stress we found, for example, that the band gaps of 3C-SiCNWs increase while the band gaps of 4H-SiCNWs with larger diameters decrease. Finally, comparing the energy positions of the valence band maximum and the conduction band minimum of the SiCNWs with different polytypes, we estimate the band offsets for homostructures of SiCNWs. We found that 3C/4H and 3C/6H SiCNWs homostructures present a type-I band alignment, with both electrons and holes lying in the 3C-SiCNW layers.

## V. ACKNOWLEDGMENTS

All calculations were performed using the computational facilities of CENAPAD/SP, Brazil. J.B.O. and R.H.M. acknowledge financial support from the Brazilian agencies CNPq and FAPEMIG.

[1] R. Wu, K. Zhou, C. Y. Yue, J. Wei, and Y. Pan, Progress in Materials Science **72**, 1 (2015)
[2] H. bo Lu, B. C. Y. Chan, X. Wang, H. T. Chua, C. L. Raston, A. Albu-Yaron, M. Levy, R. Popowitz-Biro, R. Tenne, D. Feuermann, and J. M. Gordon, Nanotechnology **24**, 335603 (2013)
[3] Z. Pan, H.-L. Lai, F. C. K. Au, X. Duan, W. Zhou, W. Shi, N. Wang, C.-S. Lee, N.-B. Wong, S.-T. Lee, and S. Xie, Adv. Mater. **12**, 1186 (2000)
[4] G. Shen, D. Chen, K. Tang, Y. Qian, and S. Zhang, Chem. Phys. Lett. **375**, 177 (2003)
[5] W. Zhou, X. Liu, and Y. Zhang, Appl. Phys. Lett. **89**, 223124 (2006)
[6] J. J. Niu and J. N. Wang, J. Phys. Chem. B **111**, 4368 (2007)
[7] G. Z. Yang, H. Cui, Y. Sun, L. Gong, J. Chen, D. Jiang, and C. X. Wang, J. Phys. Chem. C **113**, 15969 (2009)
[8] X. Luo, W. Ma, Y. Zhou, D. Liu, B. Yang, and Y. Dai, Nanoscale Res. Lett **5**, 252 (2010)
[9] H.-K. Seong, H.-J. Choi, S.-K. Lee, J.-I. Lee, and D.-J. Choi, Appl. Phys. Lett. **85**, 1256 (2004)
[10] K.-Z. Li, J. Wei, H.-J. Li, Z.-J. Li, D.-S. Hou, and Y.-L. Zhang, Mat. Sci. Eng. A **460-461**, 233 (2007)
[11] J. Wei, K. Li, H. Li, D. Hou, Y. Zhang, and C. Wang, J. Alloys Compd. **462**, 271 (2008)
[12] D.-W. Kim, Y.-J. Choi, K. J. Choi, J.-G. Park, J.-H. Park, S. M. Pimenov, V. D. Frolov, N. P. Abanshin, B. I. Gorfinkel, N. M. Rossukanyi, and A. I. Rukovishnikov, Nanotechnology **19**, 225706 (2008)
[13] Y. Yang, G. Meng, X. Liu, L. Zhang, Z. Hu, C. He, and Y. Hu, J. Phys. Chem. C **112**, 20126 (2008)
[14] E. W. Wong, P. E. Sheehan, and C. M. Lieber, Science **277**, 1971 (1997)
[15] X. D. Han, Y. F. Zhang, K. Zheng, X. N. Zhang, Z. Zhang, Y. J. Hao, X. Y. Guo, J. Yuan, , and Z. L. Wang, Nano Lett. **7**, 452 (2007)
[16] W. Yang, H. Araki, C. Tang, S. Thaveethavorn, A. Kohyama, H. Suzuki, and T. Noda, Advanced Materials **17**, 1519 (2005)
[17] W. Nhuapeng, W. Thamjaree, S. Kumfu, P. Singjai, and T. Tunkasiri, Current Applied Physics **8**, 295 (2008), aMN-3 (Third International Conference on Advanced Materials and Nanotechnology)Third International Conference on Advanced Materials and Nanotechnology
[18] R. Rurali, Phys. Rev. B **71**, 205405 (2005)
[19] More than 200 polytypes are known for bulk SiC. The most studied ones are the hexagonal polytypes 2H, 4H, 6H, and the cubic form 3C (or $\beta$).
[20] M. Durandurdu, Phys. Stat. Sol. (b) **243**, R37 (2006)
[21] B. Yan, G. Zhou, W. Duan, J. Wu, and B.-L. Gu, Appl. Phys. Lett. **89**, 023104 (2006)
[22] Z. Wang, M. Zhao, T. He, H. Zhang, X. Zhang, Z. Xi, S. Yan, X. Liu, and Y. Xia, J. Phys. Chem. C **113**, 12731 (2009)
[23] P. Hohenberg and W. Kohn, Phys. Rev. **136**, B864 (1964)
[24] J. M. Soler, E. Artacho, J. D. Gale, A. García, J. Junquera, P. Ordejón, and D. Sánchez-Portal, J. Phys.: Condens. Matter **14**, 2745 (2002)
[25] N. Troullier and J. L. Martins, Phys. Rev. B **43**, 1993 (1991)
[26] W. Kohn and L. J. Sham, Phys. Rev. **140**, A1133 (1965)
[27] D. M. Ceperley and B. J. Alder, Phys. Rev. Lett. **45**, 566 (1980)
[28] O. F. Sankey and D. J. Niklewski, Phys. Rev. B **40**, 3979 (1989)
[29] J. J. Petrovic, J. V. Milewski, D. L. Rohr, and F. D. Gac, *Petrovic* **20**, 1167 (1985)
[30] W. R. Lambrecht, B. Segall, M. Methfessel and, M. Van Schilfgaarde, Phys. Rev. B **44**, 3685 (1991)
[31] G. L. Harris, *Properties of Silicon Carbide* (Institution of Engineering and Technology, London, 1995)
[32] W. A. Harrison, *Electronic Structure and the Properties of Solids* (Dover, 1989)
[33] O. Auciello, J. Birrell, J. A. Carlisle, J. E. Gerbi, X. Xiao, B. Peng, and H. D. Espinosa, J. Phys.: Condens. Matter **16**, R539 (2004)
[34] P. Giannozzi, S. Baroni, N. Bonini, M. Calandra, R. Car, C. Cavazzoni, D. Ceresoli, G. L. Chiarotti, M. Cococcioni, I. Dabo, A. D. Corso, S. de Gironcoli, S. Fabris, G. Fratesi, R. Gebauer, U. Gerstmann, C. Gougoussis, A. Kokalj, M. Lazzeri, L. Martin-Samos, N. Marzari, F. Mauri, R. Mazzarello, S. Paolini, A. Pasquarello, L. Paulatto, C. Sbraccia, S. Scandolo, G. Sclauzero, A. P. Seitsonen, A. Smogunov, P. Umari, and R. M. Wentzcovitch, Journal of Physics: Condensed Matter **21**, 395502 (2009)
[35] J. J. Petrovic, J. V. Milewski, D. L. Rohr, and F. D. Gac, *J. Mater. Sci.* **20**, 1167 (1985)
[36] S. Limpijumnong and W. R. L. Lambrecht, Phys. Rev. B **57**, 12017 (1998)
[37] C. H. Park, B.-H. Cheong, K.-H. Lee, and K. J. Chang, Phys. Rev. B **49**, 4485 (1994)
[38] K. J. Chang and M. L. Cohen, Phys. Rev. B **35**, 8196 (1987)
[39] M. Jiang, S. M. Peng, H. B. Zhang, C. H. Xu, H. Y. Xiao, F. A. Zhao, Z. J. Liu, and X. T. Zu, Sci. Rep. **6** (2016),

10.1038/srep20669
[40] I. S. Santos de Oliveira and R. H. Miwa, Phys. Rev. B **79**, 085427 (2009)
[41] C. Persson and U. Lindefelt, Phys. Rev. B **54**, 10257 (1996)
[42] Z. Wang, M. Zhao, T. He, X. Zhang, Z. Xi, S. Yan, X. Liu, and Y. Xia, J. Phys. Chem. C **113**, 856 (2009)
[43] T. Ito, K. Sano, T. Akiyama, and K. Nakamura, Thin Solid Films **508**, 243 (2006)
[44] G. Wang and X. Li, Journal of Applied Physics **104**, 113517 (2008)
[45] S. Cuenot, C. Frétigny, S. Demoustier-Champagne, and B. Nysten, Phys. Rev. B **69**, 165410 (2004)
[46] Y. Chen, T. Burgess, X. An, Y.-W. Mai, H. H. Tan, J. Zou, S. P. Ringer, C. Jagadish, and X. Liao, Nano Letters **16**, 1911 (2016), pMID: 26885570, http://dx.doi.org/10.1021/acs.nanolett.5b05095
[47] C. L. dos Santos and P. Piquini, Phys. Rev. B **81**, 075408 (2010)
[48] P. W. Leu, A. Svizhenko, and K. Cho, Phys. Rev. B **77**, 235305 (2008)
[49] B. Lee and R. E. Rudd, Phys. Rev. B **84**, 161303 (2011)
[50] A. J. Lee, M. Kim, C. Lena, and J. R. Chelikowsky, Phys. Rev. B **86**, 115331 (2012)
[51] M. A. Makeev, D. Srivastava, and M. Menon, Phys. Rev. B **74**, 165303 (2006)
[52] P. W. Leu, A.Svizhenko, and K.Cho, Phys. Rev. B **77**, 235305 (2008)
[53] A. Fissel, Physics Reports **379**, 149 (2003)
[54] A. Qteish, V. Heine, and R. J. Needs, Phys. Rev. B **45**, 6534 (1992)
[55] K. F. Dombrowski et. al., Appl. Phys. Lett. **65**, 1811 (1994)
[56] A. O. Evwaraye, S. R. Smith, and W. C. Mitchel, Appl. Phys. Lett. **67**, 3319 (1995)
[57] S. P. Beckman, J. Han, and J. R. Chelikowsky, Phys. Rev. B **74**, 165314 (2006)
[58] H. Zhang, Y. Xu, J. Zhou, J. Jiao, Y. Chen, H. Wang, C. Liu, Z. Jiang, and Z. Wang, J. Mater. Chem. C **3**, 4416 (2015)
[59] J. Kuang, and W. Cao, Appl. Phys. Lett. **103**, 112906 (2013)
[60] K. Pemasiri, M. Montazeri, R. Gass, L. M. Smith, H. E. Jackson, J. Yarrison-Rice, S. Paiman, Q. Gao, H. H. Tan, C. Jagadish, X. Zhang, and J. Zou, Nano Letters **9**, 648 (2009), pMID: 19170615, http://dx.doi.org/10.1021/nl802997p
[61] M. D. Moreira, P. Venezuela, and R. H. Miwa, Nanotechnology **21**, 285204 (2010)
[62] M. Amato, T. Kaewmaraya, A. Zobelli, M. Palummo, and R. Rurali, Nano Letters **16**, 5694 (2016)